Study of the Influence of Several Mordenite Modifications on Its N_2 and O_2 Adsorption Properties

Isabel Salla,[†] Pilar Salagre,*[,†] Yolanda Cesteros,[†] Francisco Medina,[‡] and Jesús E. Sueiras[‡]

Facultat de Química, Universitat Rovira i Virgili, Pl. Imperial Tarraco,1. 43005, Tarragona, Spain, and Escola Tècnica Superior d'Enginyeria Química, Universitat Rovira i Virgili, Av. Països Catalans, 26, 43007, Tarragona, Spain

Received: November 6, 2003

Na-mordenite zeolite was cation-exchanged to obtain Li-, Li/Ag- and Ag-mordenite and treated with NH_4F to obtain Na-, Li-, Li/Ag-mordeniteF (1%) and Na-mordeniteF (10%). Samples were characterized by XRD, nitrogen physisorption, ^{27}Al and ^{29}Si MAS NMR, FTIR spectroscopy, and X-ray fluorescence. Special attention was given to the presence of F^- ions in the mordenite structure. Equilibrium adsorption isotherms of high-purity components N_2 and O_2 were measured at 298 K. For the cation-exchanged mordenite samples, the adsorbed nitrogen volume is slightly higher than that obtained in other zeolites such as zeolite X with a lower Si/Al ratio. This reveals the significant influence of the cation's accessibility to the gas molecules in these adsorption processes. N_2 adsorption capacity increases in the order $Na^+ < Ag^+ < Li^+$, whereas the N_2/O_2 adsorption selectivity varies as $Na^+ < Li^+ < Ag^+$ for the cation-exchanged mordenite samples. In samples prepared by fluorinated treatment, the effect is different depending on the extraframework cation present. When Na^+ and Li^+ cations are present, F atoms decrease the shielding caused by the walls to the cation's charge resulting in an increase on the adsorption selectivity, especially at low pressures, with a slight decrease in the number of active sites. However, the effect of F on Ag^+ cations is mainly an electronegative effect, making the adsorbate−adsorbent interaction less favorable.

Introduction

Separation of nitrogen and oxygen by adsorption processes has become in the last 30 years an alternative method to cryogenic distillation because of the large energetic cost of the latter.[1,2]

Adsorption of nitrogen and oxygen in zeolites is thermodynamically controlled, and it depends on the strength of interaction between the quadrupole moment of N_2 and O_2 molecules with extraframework cations located inside the structure.[3−5] The quadrupole moment of nitrogen is three times that of oxygen. It is well-known that this separation is strongly influenced by the composition and structure of the zeolites.[6] Thus, zeolites with high aluminum content (Si/Al = 1), basically A and X, have been mainly used for air separation because of their high cation content, which is responsible for the Coulombic interaction.

Some of these zeolites have already been modified by cation exchange with alkaline and alkaline earth metals to improve the nitrogen and oxygen separation.[7−11] The factors affecting the interaction are mainly the effective charge, polarizing power, and radius of the cation. Interestingly, when Ag^+ cations interact with N_2 and O_2 molecules the bonding is a result of two contributions: the donation of the π-bond electrons to the empty s-orbital of Ag^+ and the back-donation of the d-orbital electrons of Ag^+ to the empty antibonding π-orbitals of the N_2 and O_2 molecules.[12] Because of the electron configuration of N_2 and O_2, the interaction of Ag^+ cations with N_2 becomes more favorable than with O_2.

N_2 and O_2 interactions with zeolites of low Si/Al ratio, such as zeolite X and LSX, have been highly studied by IR spectroscopy and also by quantum chemical studies using methods based on density functional theory.[8,13−19] These studies show that despite their high number of extraframework cations, not all sites are equally accessible for interaction with N_2 and O_2 molecules.[18−19] The three-dimensional porous structure of these zeolites is based in cavities, and only cations located in determined positions are susceptible to interaction with N_2 and O_2 molecules. Thus, it appears interesting to choose zeolites with porous structures with lower dimensionality where cations could be more accessible to the molecules.

Theoretical results show that extraframework cations need to have a charge of $+n.0$ (where $n = 1, 2, ...$,) to compensate for the framework's negative charge. Theoretical calculations point out that the effective charge on the cations might be reduced because of a certain shielding by partial hydration and/or the influence of framework oxygen atoms on them.[18] Introduction of elements with less polarizability in the structure, such as fluorine, should result in an increase in the total effective charge of the extraframework cations, and consequently, an increase of the interaction between cations and the quadrupole moment of N_2 and O_2 molecules could be expected.

The insertion of fluorine atoms in different zeolite and clay-type structures has been widely studied.[20−25] Several authors reported changes in the structure and catalytic properties of mordenite after activation by solutions of HF, KF, NH_4F, and F_2 and considerably higher catalytic activity in some reactions catalyzed by acids.[23,24]

Fluorination under mild conditions (e.g., with NH_4F solutions) could involve a certain dealumination, as reported by several authors. However, there are different proposals about the

* To whom correspondence should be addressed. Phone: +34 977559571. Fax: +34 977559563. E-mail: salagre@quimica.urv.es.
[†] Facultat de Química.
[‡] Escola Tècnica Superior d'Enginyeria Química.

10.1021/jp031233q CCC: $27.50
Published on Web 04/03/2004

TABLE 1: Sample Preparation Procedures

sample	starting sample	treatment
NaM	comercial	None.
LiM	NaM	Three exchanges with LiCl 2.2 M for 12 h. Vacuum filtered, washed with distilled water, and dried in a furnace at 383 K overnight.
AgM	NaM	One exchange with $AgNO_3$ 1 M for 12 h protected from light. Vacuum filtered, washed, and dried in a furnace at 383 K overnight.
Li/AgM	LiM	One exchange with $AgNO_3$ 0.01 M for 6 h protected from light. Vacuum filtered, washed, and dried in the furnace at 383 K overnight.
NaM*x*F ($x = 1, 10$)	NaM	Repeated NH_4^+ exchange with NH_4Cl 2.2 M and calcined at 673 K for 12 h.
	HM	In tefflon flasks by exchanging 1 g of H-mordenite with 50 mL of NH_4F, 8.8 mM and 0.105 M, respectively ($x = 1, 10$). After impregnation the samples were vacuum filtered and washed with distilled water.[a]
	HM*x*F ($x = 1, 10$)	Bubbling a flow of NH_3/Ar through it.
	NH_4MFx	Cation exchanged several times with NaCl 2.2 M. Vacuum filtered and washed with distilled water until free of chlorides and dried in a furnace at 383 K overnight.
LiM1F	NaM1F	Several exchanges with LiCl 2.2 M. Vacuum filtered, washed, and dried in the furnace at 383 K overnight.
Li/AgM1F	LiM1F	One exchange with $AgNO_3$ 0.01 M 6 h protected from light. Vacuum filtered, washed, and dried in the furnace at 383 K overnight.

[a] Concentrations and volumes were calculated in such a way that the % w/w of F introduced per gram of zeolite was 1 and 10.

location of fluorine after treatment. Some authors have discussed two possible reactions for the fluoride treatment:

$$\text{zeoliteOH} + \text{F}^-(\text{aq}) \rightarrow \text{zeoliteF} + \text{OH}^-(\text{aq}) \quad (1)$$

$$\text{zeoliteOH} + \text{F}^-(\text{aq}) \rightarrow \text{AlF}_x\text{OH}_y \text{ zeolite} \rightarrow \text{AlF}_3(\text{aq}) + \text{zeolite}^- \quad (2)$$

Thus, Kowalak et al.[23,24] reported the incorporation of fluorine in the framework (reaction 1) whereas Breck et al.[25] and, subsequently, Panov et al.[20] proposed the formation of extra-framework aluminum fluoride species (reaction 2). When the fluorination conditions used in these studies are examined, it seems clear that reaction 2 is more favored when using high fluorine concentrations (>3% w/w) as well as calcining at high temperatures (>450 °C).

No studies of fluorinated zeolites are reported for separation processes.

In this work, we study the N_2 and O_2 adsorption properties of mordenite. This material is the natural zeolite with the lowest Si/Al ratio (6.5 in our sample). It has a two-dimensional structure, which actually works as a one-dimensional channel system formed by 12-ring and 8-ring channels, leading probably to a better accessibility of the extraframework cations to the adsorbate molecules. Besides, we want to increase the charge location of different cations (Na^+, Li^+, and Ag^+) by introducing less-polarizing atoms of fluorine in the framework channels of the mordenite in order to improve its adsorption properties.

Experimental Section

Starting Materials. Commercial Na-mordenite (Si/Al = 6.5, CBV 10A lot no. 1822-50), designated as NaM, was used as the starting material. It was supplied by Zeolist as a hydrated powder. Its chemical composition was a SiO_2/Al_2O_3 mole ratio of 13 and a Na_2O wt % of 6.6. Lithium chloride (LiCl, 99% min, Prolabo), sodium chloride (NaCl, 99% min, Prolabo), silver nitrate ($AgNO_3$, 99.8% min, Prolabo), ammonium chloride (NH_4Cl, 99% min, Prolabo), ammonium fluoride (NH_4F, high purity, Probus), and ammonia solution (NH_3, 28%, Prolabo) were used in the preparation of the ion-exchange solutions.

Sample Preparation. The treatments used to prepare the different samples are shown in Table 1.

Characterization Techniques. *N_2 Adsorption Isotherms.* Nitrogen adsorption isotherms at 77 K and BET surface areas were obtained using a Micromeritics ASAP 2000 surface analyzer with a value of 0.164 nm^2 for the cross section of the nitrogen molecule. Specific surface areas were obtained from the BET equation.

Powder X-ray Diffraction. Powder X-ray diffraction patterns of the samples were obtained with a Siemens D5000 diffractometer (Bragg−Brentano parafocusing geometry and vertical $\theta-\theta$ goniometer) fitted with a curved graphite diffracted-beam monochromator, incident and diffracted-beam Soller slits, a 0.006° receiving slit, and a scintillation counter as a detector. The angular 2θ diffraction range was between 5° and 70°. The data were collected with an angular step of 0.05° at 3 s per step and sample rotation. Cu Kα (1.542 Å) radiation was obtained from a copper X-ray tube operated at 40 kV and 30 mA. The cell parameters and cell volume values were calculated using a matching profile with TOPAS 2.0 software (Bruker AXS).

^{27}Al and ^{29}Si MAS NMR Spectroscopy. Spectra were obtained at a frequency of 400 MHz by spinning at 5 kHz. The pulse duration was 2 μs, and the delay time was 5 s. High-purity octahedral hexahydrated aluminum chloride $AlCl_3 \cdot 6H_2O$ in its solid state and silicon nitride Si_3N_4 were used as the chemical shift reference for aluminum and silicon, respectively.

DRIFTS Investigations. Infrared spectra were recorded using an FTIR Bruker Equinox 55 instrument in the frequency range of 400−4000 cm^{-1} with a spectral resolution of 4 cm^{-1}. An MCT detector was used. Samples mixed with KBr were placed on a DRIFT cell connected to a temperature controller. Spectra of the dehydrated samples were taken after activation at 673 K for a minimum of 4 h under an Ar flow of 2 mL/s.

X-ray Fluorescence. X-ray fluorescence was used to determine the atom distribution maps and the Si/Al ratio of the fluorinated and nonfluorinated samples. Experiments were performed on a scanning electron microscope, JEOL JSM6400, operating at an accelerating voltage of 15 kV and work distances of 15 mm. All samples were covered with a graphite layer. The accumulating time for mapping experiments was around 120 s.

TABLE 2: N_2 Physisorption Characterization of Several Samples

sample	surface area (m^2/g)	micropore surface area (m^2/g)	nonmicropore surface area (m^2/g)	micropore/ nonmicropore
NaM	352	321	31	10.35
NaM1F	334	303	31	9.77
NaM10F	370	320	50	6.40

Cation Exchange Capacity (CEC). The cation exchange capacity (CEC) of different samples was determined in a way similar to that proposed by Bergaya et al.[26] First, mordenite samples were exchanged with an aqueous solution of $CuSO_4$ for 6 h at room temperature. Then, the samples were centrifuged and washed with distilled water several times. The amount of Cu^{2+} exchanged was determined by UV−vis spectroscopy at 809 nm. The CEC in meq/100 g of zeolite was calculated as the difference in concentration between the starting solution and the final solution obtained after the exchange.

N_2 and O_2 Adsorption Measurements. Adsorption isotherms were measured using a static volumetric system Micromeritics ASAP-2010. The gases used were high-purity (99.999%) N_2 and O_2. Both gases were supplied by Carburos Metálicos.

Experiments were made using an amount of sample between 0.20 and 0.30 g. The sample was contained in a quartz cup and previously activated before the adsorption measurements at 623 K using a turbomolecular vacuum pump until a pressure lower than 1 μm Hg was achieved. It is known that small amounts of molecular water inside the framework of the aluminosilicates seriously affect the adsorption capacity of these materials.[27] Adsorption measurement isotherms were performed at 298 K in the range of pressures between 0.05 and 760 mm Hg.

Results and Discussion

Sample Characterization. Nitrogen adsorption isotherms obtained at 77 K were classified as type I for all samples, which corresponds to microporous materials according to the BDDT classification.[28] The BET surface area of the starting sample was around 350 m^2/g. Sample modifications by cation exchange do not modify porosity and surface area results. In contrast, the fluorination of mordenite with NH_4F causes structural variations which results in a slight increase of its meso−macro porosity (see Table 2), but it does not practically affect the isotherm shape. These results are in agreement with the dealumination detected by other techniques for these samples, as commented below.

Figures 1 and 2 show the ^{27}Al and ^{29}Si MAS NMR spectra, respectively, for several samples. ^{27}Al NMR of the starting mordenite (NaM) and the low-fluorinated mordenite (NaM1F) show that the aluminum is mainly tetrahedrally coordinated since only one peak at 50 ppm can be observed. However, for the highly fluorinated material (NaM10F), besides this tetrahedral aluminum, a broad band around 0 ppm indicates the presence of some octahedral aluminum. Therefore, fluorination under mild conditions does not cause an appreciable dealumination of the structure when the amount of fluorine used is low (1% w/w). This has also been suggested by Kowalak et al.[23] Otherwise, when the amount of fluorine is higher (10% w/w) part of the tetrahedral aluminum becomes octahedrally coordinated. This peak confirms the framework dealumination, which is responsible for the new mesoporosity observed from physisorption data.

From the ^{29}Si NMR results (Figure 2), the starting mordenite and the low-fluorinated mordenite show three bands at −115 ppm, −105 ppm, and −100 ppm (less intense) which correspond to the Si coordinated to 0 Al, 1 Al, and 2 Al, respectively. The ^{29}Si NMR spectra for the NaM and NaM1F samples are very similar with a very slight decrease of the band at −105 ppm for NaM1F, which indicates a few dealuminations not observed before by ^{27}Al NMR. For the NaM10F sample, this band at −105 ppm tends to disappear, increasing the band at −115 ppm. From these results, we can suggest that the dealumination observed is mainly produced by the initial attack of fluorine on the SiOHAl groups of its acidic form (HM10F).

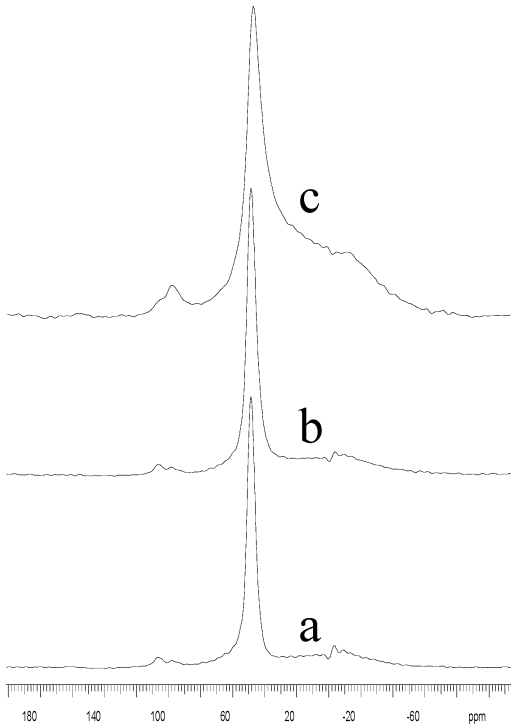

Figure 1. ^{27}Al MAS NMR spectra for (a) NaM, (b) NaMF1, and (c) NaMF10 samples.

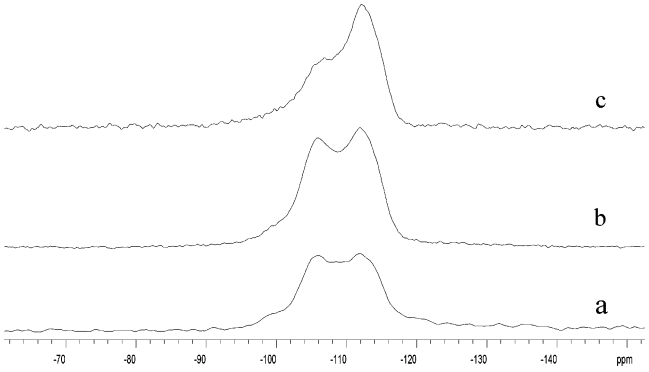

Figure 2. ^{29}Si MAS NMR of (a) NaM, (b)NaM1F, and (c) NaM10F.

X-ray powder diffraction patterns of mordenite samples before and after fluorination were taken. The samples, which show similar crystallinity, were identified as mordenite. Additionally, no other phases were detected although the ^{27}Al MAS NMR spectra showed the presence of octahedral aluminum for the highly fluorinated sample (NaM10F), as reported above.

Nevertheless, some structural modifications have been detected as reflected in the variation of the cell parameters calculated from the diffraction patterns (see Table 3). The cell volume practically does not change for the NaM1F sample with respect to the nonfluorinated sample (NaM), whereas there is a significant decrease in the cell volume value for the sample NaM10F. However, the cell parameter values do not change in

TABLE 3: Cell Parameters of NaM, NaM1F, and NaM10F Samples Calculated by XRD

sample	*a* (Å)	*b* (Å)	*c* (Å)	cell volume (Å^3)
NaM	18.103(4)	20.451(3)	7.514(1)	2782
NaM1F	18.113(4)	20.437(3)	7.512(1)	2781
NaM10F	18.181(4)	20.383(3)	7.490(1)	2775

the same direction since parameter *a* increases whereas parameters *b* and *c* decrease when increasing the fluorine treatment. These different tendencies are a consequence of several factors such as the incorporation of fluorine in the structure as well as the dealumination of samples but are also a consequence of the presence of extraframework aluminum in the channels of the mordenite. Therefore, we think that the decrease observed in the cell volume for sample NaM10F should be mainly due to both dealumination and incorporation of the fluorine in the structure.

To confirm this behavior, the IR spectra of HM, HM1F, and HM10F samples were also taken. Figure 3 shows the FTIR spectra in the region between 3800 and 3500 cm^{-1}. For the nonfluorinated sample (HM) two peaks are observed at 3740 and 3645 cm^{-1}. The first corresponds to SiOH terminal groups and the second corresponds to SiOHAl groups although the presence of silanol groups related to structural defects cannot be discarded.[29] After fluorination, some changes are observed in the FTIR spectra of that region, especially with respect to the band at 3645 cm^{-1} since the band at 3740 cm^{-1} almost does not change for both samples. This make us think that the attack of fluorine practically does not affect the terminal silanol groups.

For the HM1F sample, a new band appears at 3614 cm^{-1}. We think that this band corresponds to the same bridged groups of that of the 3645 cm^{-1} band observed for the nonfluorinated sample. It shifts to lower wavenumber probably because of the effect of the fluorine introduced inside the structure, which makes them more acidic. The shift observed is in agreement with the appearance of framework species **1**, previously proposed by Kowalak et al.[23,24]

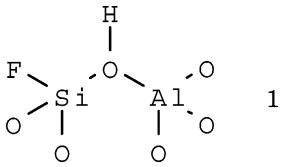

1

Also, a less intense band was observed for this sample around 3650 cm^{-1}, which should correspond to the original SiOHAl groups.

For the sample HM10F, more important changes are observed. The first is the appearance of a more intense band at 3655 cm^{-1}. From the results obtained by ^{27}Al NMR for this sample, and together with the data found in the literature,[24] this band can be attributed to AlOH nonframework groups formed as a consequence of the dealumination. Second, there is a band at 3580 cm^{-1} which could be explained in a similar way as that for the band observed at 3614 cm^{-1} for the HM1F sample. In this case, the higher red shift of the SiOHAl groups band could be due to the presence of stronger Brönsted sites, associated with the more extensive fluorination suffered by NaM10F, although the interaction of these groups with some Al−F species formed during dealumination in the intracrystalline space probably contributes to this shift.[30]

Moreover, the shift in the position for the symmetric and asymmetric TO_4 tetrahedra bands in the mid-IR region (see Table 4) is almost the same for the nonfluorinated (NaM) and the low-fluorinated (NaM1F) structures but shifts toward higher frequencies for the highly fluorinated sample (NaM10F), confirming the dealumination of the structure.

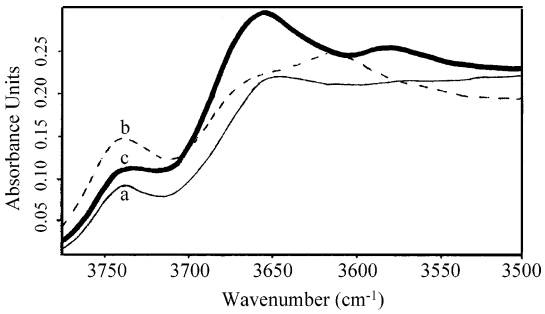

Figure 3. FTIR spectra of (a) HM, (b) HM1F, and (c) HM10F samples.

TABLE 4: IR Frequencies of Fluorinated Mordenites, CEC, and Si/Al Ratio Determined by X-ray Fluorescence

sample	IR frequencies (cm^{-1}) ν_{as}(T−O)	IR frequencies (cm^{-1}) ν_s(T−O)	CEC (meq/100 g)	Si/Al ratio
NaM	1064	630	240	7.0
NaMF1	1065	629	217	7.4
NaMF10	1072	637	52	8.2

TABLE 5: N_2/O_2 Adsorption Selectivity at 298 K at Different Pressures

sample	selectivity[a] 760 mm Hg	345 mm Hg	50 mm Hg
NaM	2.8	3.3	4.1
NaMF10	2.0	2.2	2.3
NaMF1	2.8	3.4	4.6
LiM	3.0	4.0	6.6
LiMF1	2.9	4.0	7.2
LiAgM	2.8	4.0	7.3
LiAgMF1	3.0	3.9	6.3
AgM	3.3	4.3	10.2

[a] N_2/O_2 adsorption selectivity was defined as the ratio of the volume adsorbed of N_2 and the volume adsorbed of O_2 at the given pressure.

Finally, to complete the characterization of the samples, X-ray fluorescence element map distributions (not shown here) of Si, Al, and Na were also performed and the Si/Al ratio was determined by X-ray fluorescence for some samples. Si, Al, and Na map distributions showed a homogeneous atomic distribution in all cases. Quantification results, expressed as the Si/total Al (framework + extraframework) ratio (Table 4), indicate that in addition to what was observed by other techniques, there is an initial loss of aluminum during the fluorination treatment, which is higher when a higher amount of NH_4F is used. The same tendency was observed in the CEC values (Table 4). The more important decrease observed for the NaM10F sample is in agreement with the presence of extraframework $[Al(OH)_{3-x}]^{x+}$groups, hardly exchangeable, which are responsible for the neutralization of the framework charge.

N_2 and O_2 Adsorption Measurements. Nitrogen and oxygen adsorption isotherms are shown in Figures 4, 5, and 6 for different samples. The adsorption volume values are referred to the weight of sample before activation (cm^3/g). The N_2/O_2 selectivity results are listed in Table 5. N_2/O_2 selectivity was calculated as the ratio between the volume of N_2 adsorbed and the volume of O_2 adsorbed at three given pressures (760, 345, and 50 mm Hg).

From the results exhibited in Figure 4 and Table 5, for the nonfluorinated samples it can be observed that substitution of

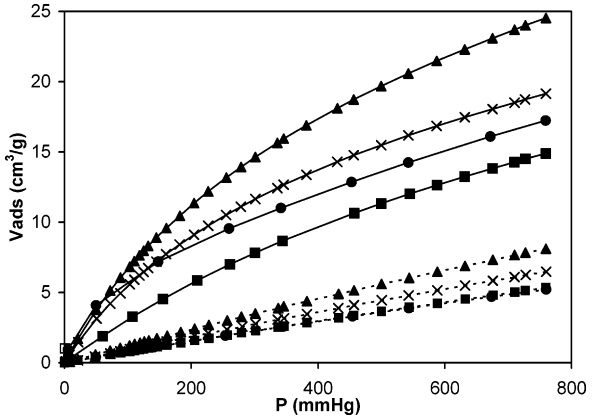

Figure 4. Equilibrium isotherms of N_2 (upper) and O_2 (lower) at 298 K on NaM (■), LiM (▲), Li/AgM (×), and AgM (●).

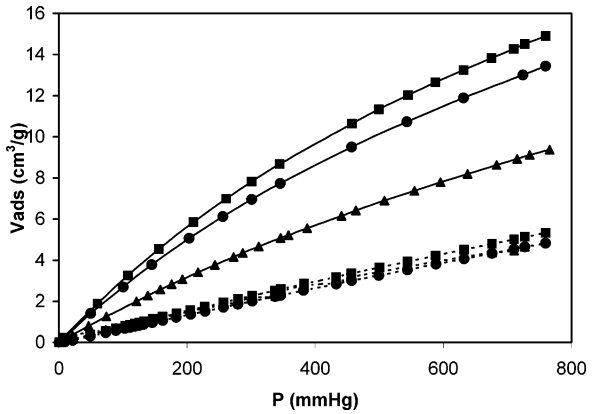

Figure 5. Equilibrium isotherms of N_2 (upper) and O_2 (lower) at 298 K on NaM (■), NaMF1 (●), and Na MF10 (▲).

Na^+ cations by Li^+ cations leads to an increase in the adsorption volume, and besides, there is also an increase in the N_2/O_2 adsorption selectivity. This is attributed to the major charge/radius ratio of Li^+, which favors the electrostatic interaction with the adsorbate molecules.[6]

Interestingly, the adsorption volumes obtained for these Na-mordenite and Li-mordenite samples are slightly higher than those reported in the literature[12] for NaX and LiX samples, respectively, with comparable selectivity values. This reveals the importance of the accessibility of the cations for the gas molecules and confirms our expectations about the use of a zeolite with less cation content but more accessibility.

On the other hand, when Na^+ cations are substituted by Ag^+ cations in the mordenite, the isotherm shape becomes less linear (Figure 4). This has also been observed in other Ag-exchanged zeolites,[12] where the N_2/O_2 selectivity increases specially at low pressures. In contrast, we observe a smaller increase in the total volume adsorbed for the AgM sample with respect to that reported for other Ag-exchanged zeolites. This can be attributed to the different degrees of complexation interactions, since it is well-known that these interactions are strongly influenced by the nature of the zeolite.[31,32]

The adsorption results obtained after the fluorination procedures are shown in Figures 5 and 6 and in Table 5. NaM1F and LiM1F show similar behavior with respect to the volume adsorbed and the adsorption selectivity results. The total volume adsorbed decreases in both cases after fluorination. This could be explained by a slight decrease in the number of active sites, because some dealumination takes place when the amount of fluorine introduced is low, according to the Si/Al ratio and CEC values (Table 4). Interestingly, these results also show an

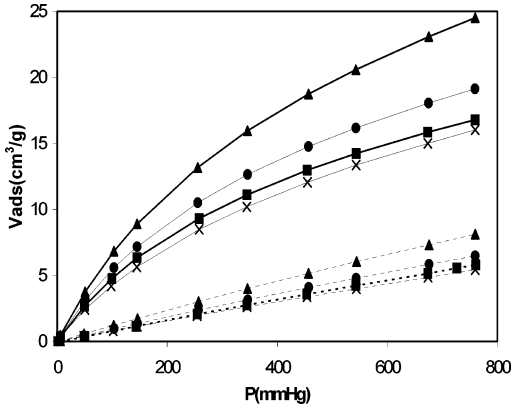

Figure 6. Equilibrium isotherms of N_2 (upper) and O_2 (lower) at 298 K on LiM (▲), LiM1F (■), LiAgMF (●), and LiAgM10F (×).

increase in selectivity preferentially at low pressures for both samples. This indicates a smaller shielding of cations when F atoms are incorporated inside the mordenite structure, because of the less-polarizable character of fluorine, although probably, fluorination only affects the more accessible surface.

On the other hand, for the NaM10F sample, with more fluorine introduced, both the volume adsorbed and the adsorption selectivity decrease sharply due to the higher dealumination and the presence of hardly exchangeable $[Al(OH)_{3-x}]^{x+}$groups, which should scarcely have the capacity for quadrupolar interaction. This involves a considerable decrease in the number of active sites.

Otherwise, the introduction of small amounts of fluorine in the presence of Ag^+ cations (sample LiAgM1F) results in a decrease both in the volume adsorbed and on the N_2/O_2 selectivity. This can be explained by the effect of the high electronegativity and low polarizability of the fluorine atoms, which cause a decrease in the π-complexation interactions between the cations Ag^+ and the N_2 and O_2 molecules.

A study reported by Yang et al.[33] about the adsorption of oxygen and nitrogen on silver halides revealed that the polarization effect can influence the 5s orbital energies of Ag. In fact, the difference in energy between the highest occupied molecular orbital (HOMO) of the adsorbate and the lowest unoccupied molecular orbital (LUMO) of the adsorbent increases when the polarizability of the halide decreases, and consequently, the presence of fluorine probably contributes to a weaker adsorbate−adsorbent interaction, although unimportant differences between N_2 and O_2 can be expected. However, the electronegativity of fluorine atoms would "attract" the electronic density from the Ag, and consequently, this reduces the contribution of back-donation. This reduction affects nitrogen more because its two π*-antibonding orbitals are empty, whereas those of oxygen are occupied by one electron each. This explains the decrease in the N_2/O_2 selectivity.

Conclusions

Mordenite, despite its Si/Al ratio of 6.5, can adsorb slightly higher volumes of N_2 than zeolites with a lower Si/Al ratio, maintaining high N_2/O_2 selectivity. This behavior can be explained because its two-dimensional porous structure in channels makes cation accessibility easier than in zeolites based on cavities. Therefore, this natural zeolite is a good alternative to synthetic zeolite X for the N_2/O_2 separation process.

In samples prepared by cation exchange, the volume of N_2 adsorbed increases as $Li^+ > Ag^+ > Na^+$, and the adsorption selectivity of N_2/O_2 increases as $Ag^+ > Li^+ > Na^+$. For samples

exchanged with Li^+ and Na^+ cations, linear isotherms typical of weak electrostatic interactions are observed, whereas for Ag^+ samples parabolic isotherms are observed as a consequence of the π-complexation interactions.

The introduction of fluorine in the structure framework is found to have a positive effect on the N_2/O_2 adsorption selectivity. Fluorination with high amounts of NH_4F involves an important dealumination, whereas fluorination with low amounts does not practically cause dealumination of mordenite and some fluorine remains inside the structure modifying the electronic properties of some cations. This fluorine results in a smaller shielding of these cations by the framework structure, which leads to an increase in the N_2/O_2 selectivity adsorption at lower pressures, despite the loss in the number of active sites.

Acknowledgment. The authors are grateful for the financial support of the Fundación Domingo Martínez and to the Generalitat de Catalunya (2002FI 00667).

References and Notes

(1) Sicar, S. *Adsorpt. Sci. Technol.* **2001**, *19*, 347.

(2) Kim, J. N.; Chue K. T.; Cho S. H. *Sep. Sci. Technol.* **1995**, *30* (3), 347.

(3) Yang, R. T. *Gas Separation by Adsorption Process*; Butterworth: Boston, MA, 1987 (reprinted by Imperial College Press: London and World Scientific Publishing Co.: River Edge, NJ, 1997); pp 9−48.

(4) Armor, J. N. Molecular Sieves for Air Separation. In *Materials Chemistry: An Emerging Discipline*; Interrante, L. V., Casper, L. A., Ellis, A. B., Eds.; American Chemical Society: Washington, DC, 1995; pp 321−334.

(5) Ruthven, D. M. *Principles of Adsorption and Adsorption Processes*; John Wiley & Sons: New York, 1984.

(6) Coe, C. G. *Access in Nanoporous Materials*; Pinnavaia, J. B., Thrope, M. F., Eds.; Plenum Press: New York, 1995.

(7) Coe, C. G.; Kirner, J. F.; Pierantozzi, R.; White, T. R. U.S. Patent 5,152,813, 1992.

(8) Pápai, I.; Goursot, A.; Fajula, F.; Plee, D.; Weber J. *J. Phys. Chem.* **1995**, *99*, 12925.

(9) Rege, S. U.; Yang, R. T. *Ind. Eng. Chem. Res.* **1997**, *36*, 5358.

(10) Chousdary, V. N.; Jasra, R. V.; Bhat, T. S. *Ind. Eng. Chem. Res.* **1993**, *32*, 548.

(11) Chao, C. C. EP Patent 0297542A2, 1998.

(12) Yang, R. T.; Chen, Y. D.; Peck, J. D.; Chen, N. *Ind. Eng. Chem. Res.* **1996**, *35*, 3093.

(13) Smudde, G. H.; Slager, T. L.; Coe, C. G.; MacDougall, J. E.; Weigel, S. J. *Appl. Spectrosc.* **1995**, *49* (12), 1747.

(14) Kazansky, V. B.; Bülow, M.; Tichomirova, E. *Adsorption* **2001**, *7*, 291.

(15) Goursot, A.; Vasilyev, V.; Arbuznikov, A. *J. Phys. Chem. B* **1997**, *101*, 6420.

(16) Shen, D.; Bülow, M.; Jale, S. R.; Fitch, F. R.; Ojo, A. F. *Microporous Mesoporous Mater.* **2001**, *48*, 211.

(17) Kazansky, V. B. *J. Mol. Catal. A: Chem.* **1999**, *141*, 83.

(18) Jale, S. R.; Búlow, M.; Fitch, F. R.; Perelman, N.; Shen, D. *J. Phys. Chem. B* **2000**, *104*, 5272.

(19) Jasra, R. V.; Choudary, N. V.; Bhat, S. G. T. *Ind. Eng. Chem. Res.* **1996**, *35*, 4221.

(20) Panov, A. G.; Gruver, V.; Fripiat, J. *J. Catal.* **1997**, *168*, 321.

(21) Sánchez, N. A.; Saniger, J. M.; d'Epinose de la Caillerie, J. B.; Blumenfeld, A. L.; Fripiat, J. *J. Catal.* **2001**, *201*, 80.

(22) Belzunce, M. J.; Mendioroz S.; Haber, J. *Clays Clay Miner.* **1998**, *46* (6), 603.

(23) Becker, K. A.; Kowalak, S. *J. Chem. Soc., Faraday Trans. 1* **1985**, *81*, 1161.

(24) Kowalak, S.; Khodakov, A. Y.; Kustov, L. M.; Kazanky, V. B. *J. Chem. Soc., Faraday Trans.* **1995**, *91* (2), 385.

(25) Breck, D. W.; Skeels, G. W. Proceedings of the Sixth International Congress on Catalysis, Imperial College, London, 12−16 July, 1976; Bond, G. C., Wells, P. B., Tompkins, F. C., Eds.; The Chemical Society: London, 1977; Vol. 2, p 645.

(26) Bergaya, F.; Vayer, M. *Appl. Clay Sci.* **1997**, *12*, 275.

(27) Hutson, N. D.; Zajic, S. C.; Yang, R. T. *Ind. Eng. Chem. Res.* **2000**, *39*, 1775.

(28) Gregg, S. J.; Sing, K. S. W. *Adsorption, Surface Area and Porosity*; Academic Press: London, 1982.

(29) Jentys, A.; Lercher, J. A. Techniques of Zeolite Characterization. In *Introduction to Zeolite Science and Practice*; van Bekkum, H., Flanigen, E. M., Jacobs, P. A., Jansen, J. C., Eds.; Elsevier: Amsterdam, 2001; pp 345−386.

(30) Becker, K. A.; Kowalak, S. *J. Chem. Soc., Faraday Trans. 1* **1986**, *82*, 2157.

(31) Wu, Z.; Han, S.; Cho, S.; Kim, J.; Chue, K.; Yang, R. T. *Ind. Eng. Chem. Res*. **1997**, *36*, 2749.

(32) Safark, D. J.; Eldridge, B. *Ind. Eng. Chem. Res.* **1998**, *37*, 2571.

(33) Chen N.; Yang, R. T. *Ind. Eng. Chem. Res.* **1996**, *35*, 4020.